

Interfacial dilational rheology of molecular films in dc electric fields

Sameer Mhatre,^{*,†,‡} Sébastien Simon,[†] and Johan Sjöblom[†]

[†]*Ugelstad Laboratory, Department of Chemical Engineering, Norwegian University of Science and Technology (NTNU), NO-7491 Trondheim, Norway*

[‡]*Department of Chemical and Biological Engineering, University of British Columbia, Vancouver, BC V6T 1Z3 Canada*

E-mail: sameer.mhatre@ubc.ca

Abstract

Abstract In this work we present a novel technique to measure the interfacial dilational rheology of a molecular film adsorbed at a water-oil interface in a dc electric field. A film of a highly polar sub-fraction of asphaltenes was allowed to adsorb at a water drop interface, surrounded by an organic phase and subjected to a dc electric field. The measurements involved calculations of the dynamic interfacial tension (IFT), while the drop was sinusoidally oscillated, using our in-house axisymmetric drop shape analysis (ADSA) algorithm adapted for electric fields. The amplitude of the IFT waveform over equilibrium IFT and the phase difference from the applied area oscillations were used in the estimation of surface moduli. The asphaltene films were found to become more elastic on increasing bulk concentrations and electric field strengths. However, the effect was not monotonous and observed to be governed by combinations of these parameters. The Lucassen-van den Tempel (LVDT) model was used to further elucidate the experimentally obtained interfacial dilational moduli.

Introduction

The rheological properties of liquid interfaces play a crucial role in emulsion-based products including food products, cosmetics, pharmaceuticals, paints, etc. as well as in industrial processes, for example, emulsion-polymerization, crude oil treatment, etc. In unit operations such as extraction, emulsification and distillation the rheological behaviour governs kinetics of the processes. Interestingly, the interfacial rheology of biofluids e.g. blood, serum, urine, etc. can be used as a diagnostic tool in medical research.¹ Majority of emulsions contain surfactants added to make it stable, either to enhance shelf life of the end product or to facilitate its end use. However, some liquids such as crude oils contain innate surface active components e.g. asphaltenes, resins, etc., responsible for interfacial and emulsion stability when emulsified with another immiscible fluid.² In either case the presence of surface active materials impart strong rheological properties and contribute to stability of the liquid interfaces. The interfacial rheology is just as important gauge in the stability analysis as the surface/interfacial tension, and one alone does not portray it completely.³

Unlike the bulk rheology, dilational rheology studies interfacial dynamics and packing of molecules at interfaces. The interfacial rheology of plane liquid interfaces and dilational rheology are essentially based on the same principle of surface/interfacial tension change while the interface is deformed.⁴ However, the rate of molecular adsorption and resultant interfacial properties can be different in dilational rheology thanks to the lower free energy of adsorption associated with the curved interfaces.^{5,6} The difference is more pronounced when the interface is put in an external electric field, where the electrohydrodynamic effects are curvature dependent.⁷ The curvature effect is nonetheless often overlooked in the surface rheology involving flat interfaces. Further, some other inherent drawbacks and limitations of using flat interface in the measurements are mentioned by Lucassen and van den Tempel.⁴ Therefore, to apply the rheological data to emulsions more accurately, the spheroidal interface is particularly important

The dilational surface rheology of surfactant monolayers involving pulsating sessile or

pendent drop has been studied extensively.^{3,8,9} It offers multiple benefits including distant recording and analysis of a drop profile, where the chances of sample contamination and the film disturbance are minimal. More importantly it allows the drop interface to equilibrate with the surface active material for as long time as needed and simultaneous monitoring of the interfacial properties.⁹ The dynamic surface/interfacial tension (IFT) data of various surfactants suggests that the time to adsorb and stabilize an interface are dependent on the molecules and their concentrations in the bulk phase.¹⁰ Therefore, a characterization method that facilitates longer monitoring is crucial. Moreover, the pendent or sessile drop in dilational rheology more closely mimic a drop in an emulsion where the phenomena such as interfacial convections and Marangoni effects are critical.

In a dilational rheology measurement the dynamic surface/interfacial tension (γ) is measured in response to sinusoidal surface area oscillations of a pendent or sessile drop.^{4,8} The periodic IFT data is used to obtain the IFT gradient with respect to the local interfacial deformation, also known as surface dilational modulus (E),

$$E = \frac{d\gamma}{d \ln(A)} \quad (1)$$

where A is the drop surface area. The surface dilational modulus is a complex number with the real part called the elastic dilational modulus (E') and the complex part is viscous dilational modulus (E'').

The interfaces with stronger viscoelastic properties can sustain external impacts and resist from breaking. The higher dilational elasticity helps the interface attain uniform interfacial tension and the stability.⁴ In the absence of electric fields (or other external influences) the properties are governed by bulk concentration and adsorption-desorption rates. In dilational rheology a sinusoidal cycle of surface compression and expansion leads to molecular desorption and adsorption respectively to maintain the equilibrium surface concentration.⁴ At the lower frequencies of the oscillations due to the adequate time to attain equilibrium

the film does not resist the deformation. Reverse can be observed at higher frequencies, where the dynamics of shape change does not allow the desorption and adsorption. Since the equilibrium time also depends on the bulk concentration, the dilational viscoelastic properties are believed to be governed by the concentration as well as the oscillation frequency.³ In this study we tried to understand how the presence of an electric field influences the film properties in addition to the concentrations and the frequencies.

The interfacial tension measurements in the conventional dilational rheology use Young-Laplace equation-based ADSA algorithms, which yield incorrect IFT if the drop is subjected to an external electric field.¹¹ In our previous works on interfacial tension¹¹ and adsorption dynamics¹² measurements in electric fields we demonstrated a workaround to the limitation of the conventional ADSA algorithms. Our novel ADSA algorithm which uses the Young-Laplace equation, adapted for the Maxwell stresses at the drop interface, can precisely calculate interfacial tension.¹¹ The algorithm allowed experimental investigation of the molecular adsorption dynamics at a liquid-liquid interface over a long period of time.¹² The data suggested that the field-induced streamlines around the water-oil interface resulted into a substantial increase in effective diffusion coefficient and surface excess.

The primary objective of this study is to demonstrate a step-by-step procedure to estimate dilational moduli of an interface in an electric field. The measurements of rheological properties of interfaces subjected to an electric field are critical to elucidate and design a multitude of electrohydrodynamic processes such as electrocoalescence,^{13,14} electroemulsification,¹⁵ nano-encapsulation,¹⁶ etc. Because of the abovementioned limitations in the experimental measurements, literature lacks the dilational rheological studies in multiphase systems under electric fields. However, the novel ADSA algorithm facilitated the calculation of dynamic IFT of sinusoidally pulsating drop interface under the field. We applied the method to measure the dilational interfacial viscoelastic properties of asphaltene films adsorbed at the water-oil interface of a pulsating pendent drop in an external dc electric field (E_0). The analysis was done in the light of the enhanced adsorption dynamics in

electric fields and inability of interfacial tension data to fully explain stability of liquid-liquid interfaces. The experiments were carried out at different asphaltene concentrations in the organic bulk phase and the drop shape oscillation frequencies between 0.01 and 0.05 Hz. The interface was allowed to equilibrate under a dc electric field before the shape oscillations were applied and effects of the field were studied by varying E_0 between 0.0 kV/cm and 0.833 kV/cm. The dilational viscoelastic properties were measured as a function of the electric field strength, bulk asphaltene concentration and oscillation frequency.

Experimental Methods

The experimental set-up used in this work is similar to our previous studies on dynamic interfacial tension measurements¹¹ and adsorption dynamics of surface active agents.¹² The schematics of the setup is demonstrated in Figure 1. A quartz glass cell is fitted with two horizontal plate electrodes (stainless steel, 25 mm \times 25 mm \times 1 mm) placed 24 mm apart. The upper electrode is connected to ground and the lower to the high voltage power supply. The high voltage supply unit consists of a function generator (Agilent Technologies, Model: DSO-X 2022A) and amplifier (Trek, Model:609E-6). A teflon-coated needle (stainless steel, id = 1.1 mm and od = 2.0 mm) was used to generate a pendent drop at the centre between the electrodes. The coating was applied to isolate the needle from the upper electrode such that the drop generated at its tip was not electrified. The needle was connected to a dosing pump which precisely controlled the drop volume and volume oscillations at set frequencies.

Asphaltenes and drop pulsation

Asphaltenes are the most surface active components of a crude oil, responsible for the stability of its emulsions with water. The asphaltenes can be further fractionated based on their polarity. The sub-fraction used in this work was the most polar, called irreversibly adsorbed (IA) asphaltenes, fractionation procedure of which was previously reported by Ruwoldt et

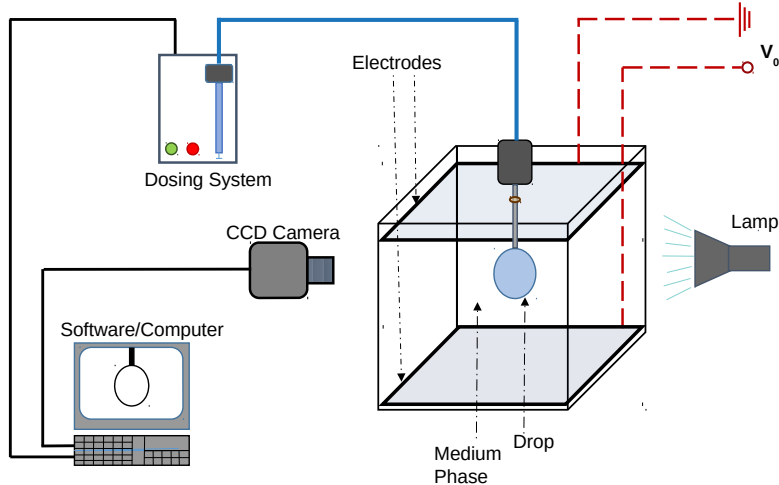


Figure 1: Schematics of the experimental setup.

al.¹⁷ Once occupied the water-oil interface IA asphaltenes do not desorb, altering the interfacial properties irreversibly.¹⁸ This also applies to the asphaltenes adsorbed under electric field, where the interfacial tension was observed to remain unchanged after switching off the field.¹²

In a typical experimental run, a Milli-Q water drop was held pendent in xylene (98.5 % VWR) containing IA asphaltenes dissolved at different concentrations ranging from 0.005 mM to 0.15 mM. The concentrations are expressed in mM throughout the manuscript considering the average molecular weight of asphaltenes 750 g/mol. The drop was kept unperturbed in a dc electric field for an hour to allow asphaltene adsorption and film formation at the water-oil interface. The time was long enough for the interface to stabilize as its interfacial tension as it showed minuscule change at longer times.¹²

Akin to the majority of dilational rheology measurements, volume of a pendent water drop was oscillated to get surface area oscillations. A 30 μl drop was oscillated by $\pm 1 \mu\text{l}$, which resulted into $\pm 2.2 \%$ surface area oscillations. However, the surface area of a drop surrounded by a surfactant solution evolves over time, increasing faster in the beginning as

the interface populates.¹⁹ Also, the presence of an electric field causes additional stretching of the drop. Depending on the concentration and the field strength the surface area attains a new value; however, it plateaus after the initial drop deformation and when the interfacial tension stops reducing. Therefore, all the dilational moduli calculations in this work are based on the drop surface area before sinusoidal shape oscillations were applied.

Dynamic interfacial tension measurement in external electric field

The method to calculate dynamic interfacial tension in a dc electric field was reported previously.¹¹ The conventional axisymmetric drop shape analysis (ADSA) algorithms used in dynamic surface/interfacial tension measurements are based on the Young-Laplace equation. The equation is a balance between pressure-drop across the interface, hydrostatic pressure and capillary pressure. Applying as it is to a drop in electric field, the Young-Laplace equation neglects the interfacial electric stresses, leading to erroneous surface/interfacial tension values. Our in-house ADSA algorithm is based on the augmented Young-Laplace equation that includes an extra term for Maxwell stresses at the drop interface. It can process tens of thousands of drop images in one go, irrespective of constant or oscillating drop volume.

The drop images were recorded at variable frame rates depending on frequency of the drop oscillation. The images were processed to obtain xy-coordinates of the drop profile; which were used in the ADSA algorithm to fit with the theoretical profiles, generated by using the Young-Laplace equation augmented for electric stresses at the drop interface.

$$\gamma\left(\frac{1}{r_1} + \frac{1}{r_2}\right) = \Delta p_0 - \Delta\rho g z + \frac{1}{2}\epsilon\mathbf{E}_n^2 \quad (2)$$

The last term in Equation 2 represents normal component of the Maxwell stresses at the drop interface. The parameters r_1 and r_2 are radii of curvatures of drop's meridian section, Δp_0 is the pressure-drop across the interface at the drop's apex, $\Delta\rho$ is the density difference, z is vertical coordinate, ϵ is electrical permittivity of the medium phase and \mathbf{E}_n is normal

component of electric field at the drop interface. The finite difference method was used to solve Laplace equation for electric potential to obtain time-dependent electric field at the drop interface. The experimental cell dimensions and instantaneous drop profiles were used in the calculations more details of which can be found elsewhere.¹¹ The theoretical profile generated using Equation 2 is matched with the experimentally obtained profile at each time step and the IFT corresponding to the best fit is calculated. The detailed algorithm can be found in reference.¹¹

Data fitting and dilational rheology

The gradient in interfacial tension with respect to the change in drop's surface area defines surface dilational modulus (E) given by equation 1. The modulus is a complex number and consists of the real part called dilational elastic modulus (E'), while the imaginary part is called dilational viscous modulus (E''),

$$E = iE' + E''. \quad (3)$$

In the experiments a pendent drop was oscillated at frequencies $f = 0.01, 0.0125, 0.0167, 0.025$ and 0.05 Hz in series. The frequencies were kept small to avoid disturbances generated due to wave-propagation⁴ and non-Laplacian drop shapes⁹ at higher frequencies. The drop undergoes five cycles of expansion and compression at each frequency beginning with the lowest frequency. As demonstrated in Figure 2(a) the reference area of the drop (A_0) - after holding the system under electric field E_0 for an hour- oscillated between $A_0 + A'$ and $A_0 - A'$, A' being the amplitude of oscillation. The interfacial tension measured during the oscillations is periodic having the same frequency but a phase difference ϕ from the area oscillations, which is attributed to the viscoelastic behaviour of the interface. The IFT waveforms have amplitude of oscillation γ , over the reference interfacial tension γ_0 , which is essentially a function of the applied frequency.

The curve fitting of the experimentally measured interfacial tension (demonstrated in Figure 2(b)) is done using the Levenberg-Marquardt algorithm. The parameters A' , γ' and ϕ are obtained from the surface area and interfacial tension curves, which are used in the calculations of the total surface dilational modulus ($|E|$), dilational elasticity modulus (E') and dilational viscous modulus (E''). The moduli are expressed in terms of A_0 , A' , γ' and ϕ as,²⁰

$$|E| = A_0 \frac{\gamma'}{A'}, \quad (4)$$

$$E' = A_0 \frac{\gamma'}{A'} \cos(\phi), \quad \text{and} \quad (5)$$

$$E'' = A_0 \frac{\gamma'}{A'} \sin(\phi) \quad (6)$$

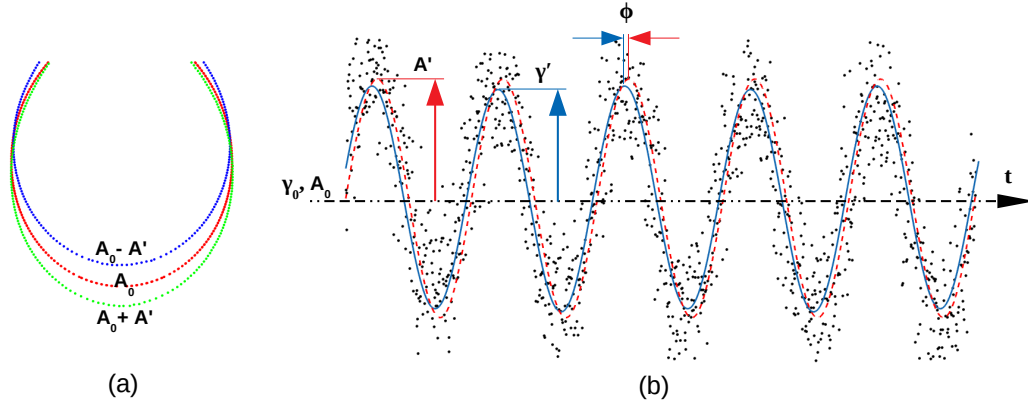


Figure 2: Illustrations of sinusoidal drop oscillations and resultant interfacial tension change. (a) Drop profiles during surface area oscillations at amplitude $\pm A'$ from reference area of A_0 . (b) Experimental interfacial tension data (\cdot) plotted along with its Levenberg-Marquardt model fit (—) and sinusoidal waveform of the drop surface area (---).

Each experiment was repeated at least four times and the dilational moduli data presented in Results and Discussion section is obtained by arithmetic averaging of at least twenty values - from five shape oscillation cycles of each four experimental runs. The error bars represent standard deviations.

Theoretical model

The interfacial dilational moduli are modelled using Lucassen - van den Tempel (LVDT) model, which works well with diffusion-controlled surface tension response to the low-frequency and small-amplitude sinusoidal area oscillations.⁴ The total surface dilational modulus (E) can be estimated as,

$$E = U \frac{1 + \xi + i\xi}{1 + 2\xi + 2\xi^2}. \quad (7)$$

Which gives the elastic and viscous dilational moduli,

$$E' = U \frac{1 + \xi}{1 + 2\xi + 2\xi^2}, \text{ and} \quad (8)$$

$$E'' = U \frac{\xi}{1 + 2\xi + 2\xi^2} \quad (9)$$

The parameters ξ and U represent a ratio of time scales for surface area change and molecular diffusion, and limiting elasticity, respectively, and are expressed as, $\xi = \frac{dC}{dT} \sqrt{\frac{D}{2f}}$ and $U = -\frac{d\gamma}{d \ln \Gamma}$. The parameters are estimated using equilibrium IFT data (γ_{eq}) and its fit to the Gibb's isotherm,

$$\Gamma = \frac{-1}{RT} \frac{d\gamma}{d \ln(C)}. \quad (10)$$

where Γ , R , T and C are surface excess, gas constant, absolute temperature and bulk phase asphaltene concentration, respectively. The diffusion coefficients (D) of asphaltenes were calculated by fitting the dynamic IFT of a freshly generated steady water-oil interface to the short time-approximation of Ward and Tordai equation.^{21,22} The D data used in the

calculations was previously reported in our article on adsorption dynamic in electric field.¹² The LVDT model predictions presented in this manuscript are calculated based on the parameters obtained after analyzing the experimental data. The model predictions got through the fitting parameters are also presented for a fair comparison .

Results and Discussion

Reference surface area

A liquid drop -freely suspended or anchored- undergoes instantaneous deformation when subjected to an electric field. Its magnitude and the newly acquired shape are governed by the field strength and electrical properties of the liquid phases, respectively.⁷ A conducting drop in an insulating medium attains a prolate shape, whereas swapping the phases results in an oblate deformation.²³ An anchored drop is observed to exhibit a gradual microscopic stretching in the presence of surface active agents regardless of the external fields. However, application of an electric field observed to intensify the deformation¹⁹ which is independent of the field direction.

In the present study, the applied field was parallel to gravity, inducing electrohydrodynamic deformation in the vertical direction, causing further increase into drop's aspect ratio. The vertical electric field helped to maintain symmetry of the drop shape, which is crucial in ADSA calculations. The maximum strength of the field that can be applied without drop breakup is determined by the electric capillary number, $Ca_E = \frac{\epsilon a E_0^2}{\gamma}$. The drop breaks when Ca_E exceed a critical value, between 0.205 and 0.215.²⁴ During the diffusion and adsorption of IA asphaltenes at water-oil interface under a dc electric field, the degree of drop deformation was collectively governed by asphaltene concentration and magnitude of the electric field. The time-dependent aspect ratios of the drop before surface area oscillations are presented in Figure .1 of Appendix A. The resultant surface area (A_0) of the stable drop after one hour is shown in Figure 3(a). The surface area increases with E_0 and the rise is propor-

tional to the bulk asphaltene concentrations when electric field was present. Although, the greater deformation and larger surface areas at higher C and E_0 are predictable, the downward trends at $C = 0.15$ mM are puzzling. The reduction might be a result of a stronger and more elastic interface that resists electrohydrodynamic deformation.

The amplitude of surface area (A'), over the reference area, at the peak and trough of an oscillation cycle shows a minor change when the drop is in an electric field (Figure 3(b)). However, the overall A' is larger under electric field and increases with asphaltene concentration. Since the drop was already in the external field before pulsation and attained maximum electrohydrodynamic deformation, the volume oscillations in a constant C solution did not yield further change in A' upon increasing E_0 . The peak surface areas were observed to remain constant at all frequencies of the oscillation. The variables A_0 and A' do not govern the measured surface dilational moduli as the calculations are based on gradient of γ during the periodic oscillations in A . However, unlike no-field measurements the calculations must be based on the surface area after electrohydrodynamic deformation of the drop.

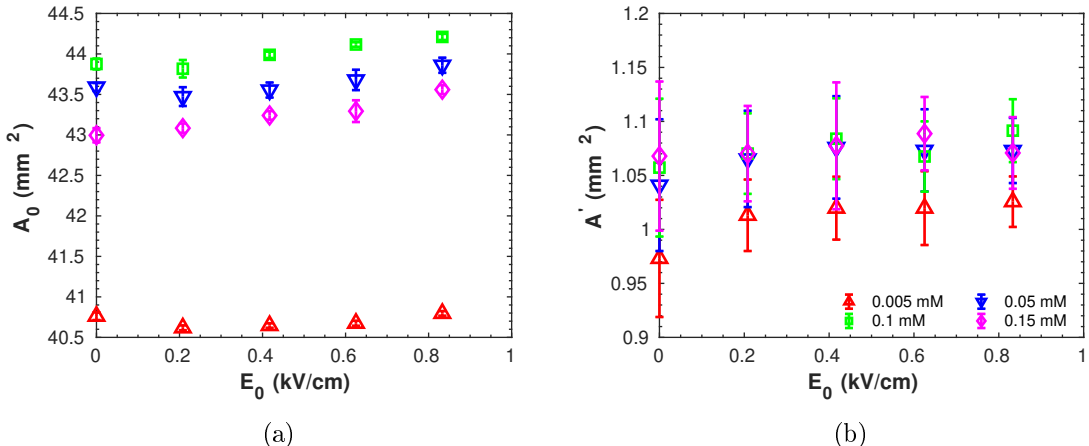


Figure 3: (a) Reference surface area of a steady water drop surrounded by asphaltene-rich organic phase under an electric field for one hour. (b) Amplitude of area oscillations above the reference surface area of the drop.

Equilibrium Interfacial Tension

The drop attains a near-constant interfacial tension upon holding static in the asphaltene solution under electric field for an hour. We call it an equilibrium interfacial tension (γ_{eq}) because no further reduction was observed and also, as demonstrated in 2 (a) γ did not show deviations in the successive cycles. The equilibrium IFT acts as a reference against which the interfacial tension sinusoidally varied during the area oscillations. Also, the reference surface areas in electric fields are governed by the equilibrium interfacial tension. The γ_{eq} data in Figure 4 demonstrates the scale of IFT reduction attributed to the externally applied electric field. The data is reproduced from our previous report on influence of external electric fields on the mass transfer dynamics at liquid interfaces.¹² At all the bulk concentrations studied, the γ_{eq} showed a sizeable reduction which was a function of the applied field strength E_0 . The decay is associated with the electric field-induced microflows around the water-oil interface, also known as electrohydrodynamic flows. The apparent diffusion coefficient (D) and, thus the surface excess of the IA asphaltenes at the interface were observed to increase steadily with E_0 .

Dilational Modulus

The total surface moduli of IA asphaltene films adsorbed at water-oil interface under external electric fields are shown in Figure 5. The $|E|$ in different concentration bulk solutions was measured by varying strength of the dc electric fields (E_0). The data, plotted against the frequency of surface area oscillations, shows that $|E|$ largely increases on increasing f with an exception of 0.005 mM solution without electric field. Since the drop was oscillated at smaller frequencies, the change appears to be steady over the frequency range studied. Similarly, the higher bulk phase concentration keeps the modulus larger regardless of the frequency. Although the concentration range used in this study i.e. 0.005 mM-0.15 mM was fairly large, further increase in the concentration might change the trends.

Similar to the equilibrium interfacial tension (Figure 4) the surface modulus shows a

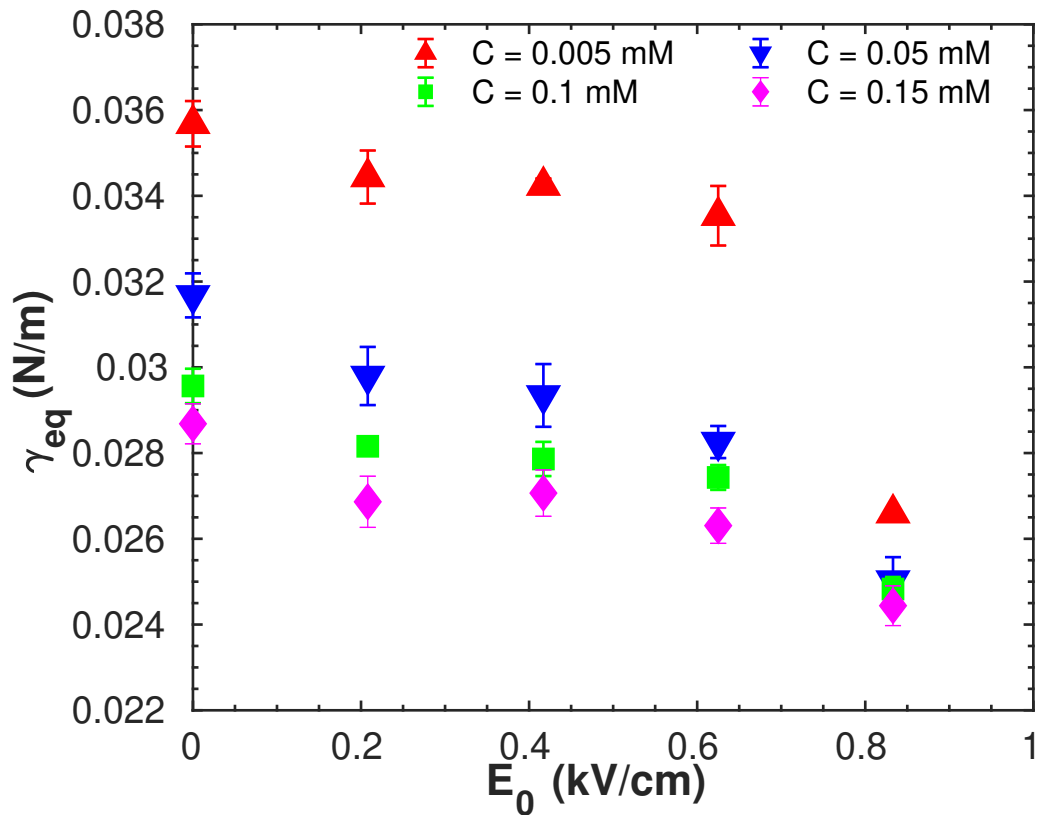


Figure 4: Equilibrium interfacial tension of water-oil interface in the presence of IA asphaltenes and external dc electric fields. γ_{eq} is calculated after holding a non-oscillating water drop in asphaltene solution of concentration C under an electric field E_0 (reproduced from Mhatre *et al.*¹²).

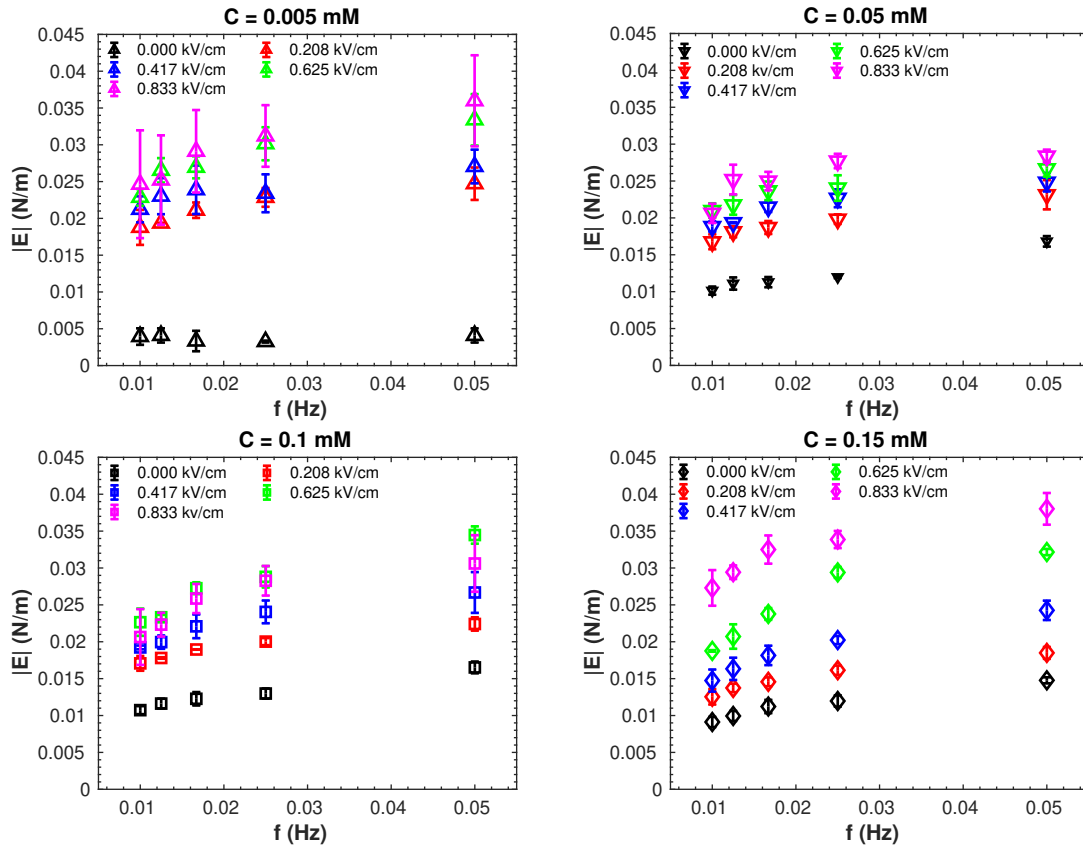


Figure 5: Total interfacial moduli of asphaltene films as a function of pulsation frequencies.

significant change when the system was put into an external electric field. A stronger electric field caused larger total modulus, which was up to 10 times larger than the no-field $|E|$ in the 0.005 mM solution. In the absence of electric field the bulk asphaltene concentrations were high enough to stabilize the water-oil interface. But, the equilibrium surface excess, estimated before application of the shape oscillations, found to boost from 2.8×10^{-6} mol/m² at no field to 4.4×10^{-6} mol/m² at 0.833 kV/cm.¹² It suggests that the interface was mostly stabilized when in the electric field.

The comparison between experimental and theoretical data is based on the parameters - U and ξ - obtained after analyzing experimental γ and γ_{eq} data, no fitting parameter was used to match the model with experimental data. For comparison we have also included the predictions obtained using fitting parameters in Figure 6(a), where it shows that the experimental and the LVDP model predictions of $|E|$ in the absence of electric field. As can be seen the predictions with fitting parameters fairly match the experimental data. However, without the fitting parameters, a discrepancy between the two is apparent, especially in the concentrated bulk solutions. The total interfacial modulus in 0.005 mM solution is in good agreement with the theoretical predictions. The estimates are distinct at the three higher concentrations, in contrast to the closely spaced experimental data. Moreover, the theoretical data is constant over the frequency range studied while the experimental data appears ramping up.

Similar discrepancies between the theoretical and experimental moduli were observed when the film was in electric fields. The deviations can be attributed to the assumption in LVDP model that the time scales of molecular diffusion and interfacial tension-change are always less than the surface area variation. In more concentrated solutions and in the presence of electric fields, the diffusion-controlled relaxation is weak. The asphaltene films seem to be insoluble, where the diffusion to and from the film during the expansion and compression respectively are negligible. The molecular diffusion, adsorption, and equilibrium between interfacial tension and subsurface concentration occur sluggishly. This may be because of

the dense packing of the films as well as the irreversibility of the asphaltene adsorption,^{12,25} which does not allow the back diffusion in to the bulk phase during compression. However, in 0.005 mM solution due to the less surface excess and thus the larger concentration gradient at the interface, the diffusion and adsorption time scales are smaller than the oscillation period. The IFT response to the drop oscillations is only due to the concentration-gradient; consequently, the experimental surface modulus conforms with the LVDP model. The theoretical predictions of $|E|$ for films in 0.15 mM solution with and without electric fields are presented in Figure .1 of Appendix B.

Although the accurate measurement of time for diffusion, adsorption and interfacial tension-change is difficult in the experiments, the theoretical ξ values and the experimental $|E|$ data can be used to correlate it to f^{-1} . The ξ data, which represents the ratio of surface area oscillation period and diffusion time scale,⁴ for the minimum and maximum oscillation frequencies and concentrations is given in Table 1. Apparently, in the majority of experiments $\xi \ll 1$ i.e. the area oscillations are significantly fast compared to the molecular diffusion at the water-oil interface. Another measure of diffusion transport during the expansion-compression cycles is the correlation between $|E|$ and \sqrt{f} , which should be linear if the interface and the bulk solution exchanged molecules during the oscillations.⁴ When scaled with $\sqrt{f/D}$, $|E|$ must be constant if plotted against the oscillation frequency. However, the non-linearity between $|E|/\sqrt{f/D}$ and f in figure 6(c) suggests the absence of diffusion while drop was pulsated. Since the apparent diffusion coefficient varies with concentration as well as the magnitude of the applied electric field, \sqrt{D} is included in the scaling.

Elastic and Viscous Moduli

The applied shape oscillations lead to the thinning of a stretched interface, where the interfacial tension at a point can be briefly higher than the nearby points. The elasticity of the film due to the spatial gradient in interfacial tension during the shape oscillations is called

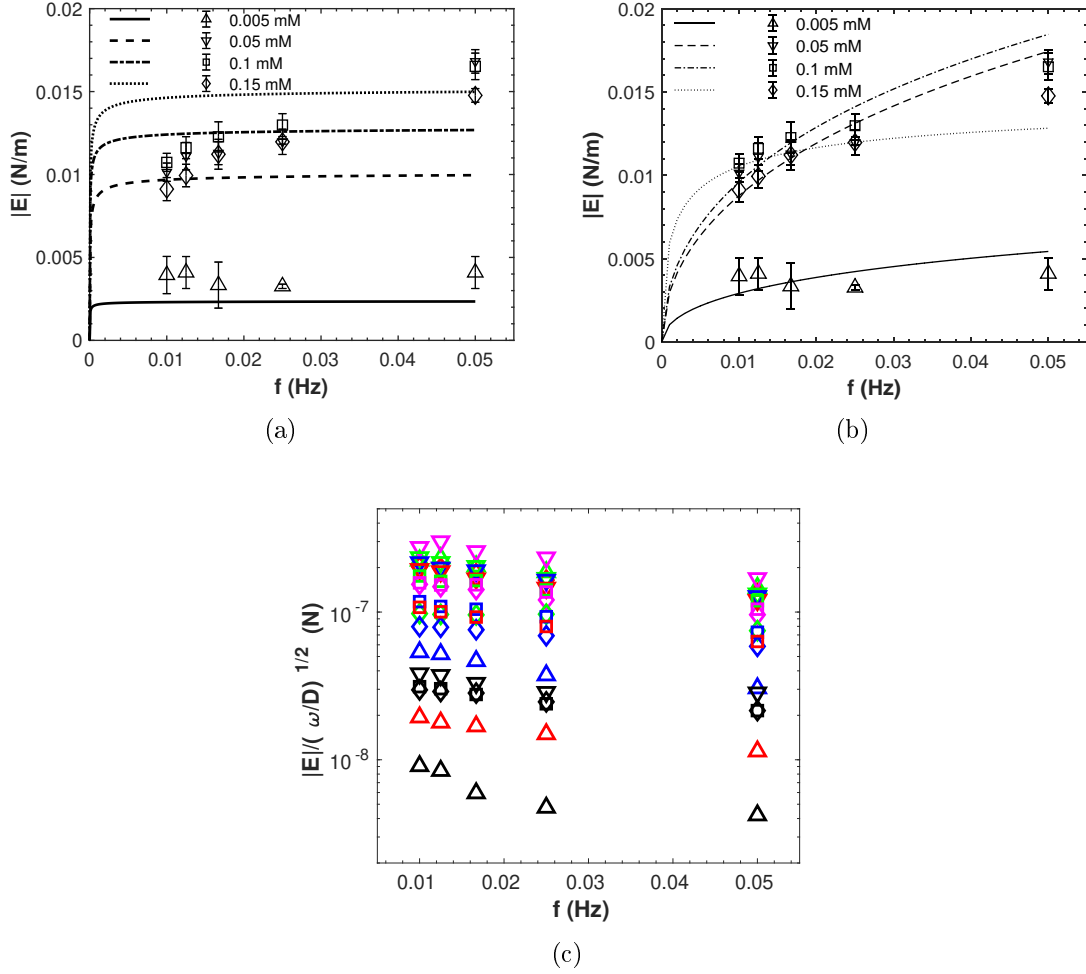


Figure 6: The experimental (symbols) and LVDP model predictions (curves) of $|E|$ for asphaltene films in the absence of electric field using (a) experimentally obtained parameters and (b) fitting parameters. (c) The experimental total interfacial modulus of Figures 5 scaled with $\sqrt{f/D}$

Table 1: ξ values at $f = 0.01$ and 0.05 Hz in 0.005 mM and 0.15 mM bulk solutions under external electric fields.

E_0 (kV/cm)	0	0.208	0.417	0.625	0.833
0.01 Hz 0.005 mM	0.03124	0.01188	0.02994	0.09398	2.618
0.01 Hz 0.15 mM	0.04353	0.1836	0.06272	0.05104	0.1378
0.05 Hz 0.005 mM	0.01397	0.005317	0.01318	0.04258	1.188
0.05 Hz 0.15 mM	0.0197	0.08276	0.02842	0.02264	0.0605

the Gibbs elasticity,²⁶ $E_{Gibbs} = 2 \times E$. The so called Plateau–Marangoni–Gibbs effect states that the newly generated surface equilibrate faster with its subsurface than the preoccupied neighboring part of the interface. The equilibration is obviously dependent on the shape oscillation frequency and on electrohydrodynamic velocity, $v_{EHD} = \frac{\epsilon E_0^2 a}{\mu}$ if the interface is subjected to an electric field. In the experimental system studied in this work, v_{EHD} ranged between 10 $\mu\text{m/s}$ and 45 $\mu\text{m/s}$.

The dilational interfacial moduli characterize resistance to the new surface generation and pace with which the interface re-establishes equilibrium. When the modulus of elasticity (E') is larger the IFT regains uniformity and drop relaxes to its original shape faster during the compression-expansion cycles. Figure 7 demonstrates the dilational elasticity and viscosity moduli in 0.005 mM and 0.15 mM solutions at $E_0 = 0.0$ kV/cm and 0.817 kV/cm. The adsorbed asphaltene films in bulk solutions with $C > 0.005$ mM (with or without electric field) were essentially elastic. When an external dc electric field was applied, the films in all solutions exhibited significantly larger elastic moduli than the viscous moduli. Interestingly, the viscous moduli remain below 5×10^{-3} N/m irrespective of the field strength, concentration or the oscillation frequency. Again, the theoretical estimates of E' and E'' under electric fields are inconsistent with the experimental measurements, and presented in Figure .1 of Appendix C for reference.

The enhanced elastic modulus in an externally applied electric field renders a liquid-liquid interface stronger. The field-dependent viscoelastic moduli have immense relevance in electric field-based multiphase treatments. For example in electrocoalescence, the boosted stability by the field would be counterproductive to the phase separation. However, we believe the reduction in interfacial tension outweighs the augmented viscoelastic properties. The interfacial stability comes into play when two drops of an emulsion come closer and a bulk phase-film separating them resists the coalescence. A bigger film is challenging to drain, where the interfacial stability is ascribed to the larger film radius.²⁷ In an electrocoalescing drop pair, the drops develop pointed leading edges when closer, which significantly reduces

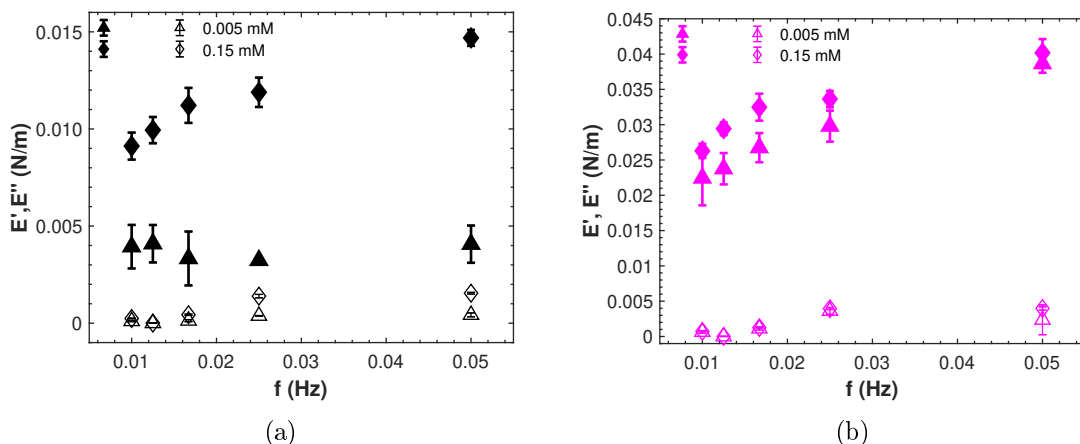


Figure 7: The experimental dilational elastic (solid symbols) and viscous (open symbols) moduli: (a) in the absence of electric field, and (b) in 0.833 kV/cm dc electric field.

the film size and resistance to the coalescence.²⁸ The stretching of drops inner faces is a result of stronger electric stresses than the interfacial tension. Further, the structural changes in the molecular film due to the phenomena such as interfacial convections, polarization and Marangoni flow may play part during the coalescence, which could be investigated in more detail in the future studies.

Conclusions

The interfacial dilational moduli of a molecular film subjected to an external dc electric field are determined by using axisymmetric drop shape analysis. A novel ADSA algorithm, adapted for electric fields, is used to calculate interfacial tension of a stable water-oil interface while it undergoes uniform sinusoidal pulsations at different frequencies. The resultant IFT waveforms follow the same frequency as the applied surface area oscillation, but with a small phase difference. The analysis of the interfacial tension waveforms and its gradient with respect to the film deformation are used to calculate interfacial dilational moduli, which describes film's response to the compression or expansion under an electric field.

We demonstrated the application of the procedure to asphaltene films, adsorbed at the

interface of a pendent water drop surrounded by an organic phase under electric fields. The interfacial dilational moduli data suggests that the films were mostly elastic irrespective of the electric field strength. The films were densely packed owing to the long aging time before the drop undergoes surface area oscillations, as well as considerable enhancement in adsorption under the fields. The films become more elastic when electric field was applied, while the viscous moduli remain low at the no-field level. The stronger films point to the magnified diffusion and adsorption rates ascribed to the symmetric microflows generated due to the fields. The data also established that the field-induced mass transport intensification strengthens the films, in addition to the interfacial tension reduction. Further, the comparison of the experimental data with theoretical predictions points to the lack of diffusion transport at interface during the shape oscillations, suggesting irreversible adsorption of asphaltenes at the water-oil interface.

Acknowledgements

The authors thank the JIP Electrocoalescence consortium “New Strategy for Separation of Complex Water-in-Crude Oil Emulsions: From Bench to Large Scale Separation (NFR PETROMAKS)”, consisting of Ugelstad Laboratory (NTNU, Norway), University of Alberta (Canada), Swiss Federal Institute of Technology in Zurich (Switzerland), Institutt for energiteknikk (Norway) and funded by Norwegian Research Council (Grant255174) and the following industrial sponsors – Nouryon, Anvendt Teknologi AS, NalcoChampion, Equinor, and Sulzer.

References

- (1) Fainerman, V. Adsorption kinetics from concentrated micellar solutions of ionic surfactants at the water-air interface. *Colloids and Surfaces* **1992**, *62*, 333–347.

- (2) Sjöblom, J.; Oye, G.; Glomm, W.; Hannisdal, A.; Knag, M.; Brandal, O.; Ese, M.; Hemmingsen, P.; Havre, T. E.; Oschmann, H.-J.; Kallevik, H. *Modern characterization techniques for crude oils, their emulsions, and functionalized surfaces.*; CRC Press: Boca Raton FL, 2006.
- (3) Stubenrauch, C.; Miller, R. Stability of Foam Films and Surface Rheology: An Oscillating Bubble Study at Low Frequencies. *The Journal of Physical Chemistry B* **2004**, *108*, 6412–6421.
- (4) Lucassen, J.; van den Tempel, M. Dynamic measurements of dilational properties of a liquid interface. *Chemical Engineering Science* **1972**, *27*, 1283–1291.
- (5) Farrow, R., M; Camp, J., P; Dowding, J., P; Lewtas, K. The effects of surface curvature on the adsorption of surfactants at the solid–liquid interface. *Phys. Chem. Chem. Phys.* **2013**, *15*, 11653–11660.
- (6) Komura, S.; Hirose, Y.; Nonomura, Y. Adsorption of colloidal particles to curved interfaces. *The Journal of Chemical Physics* **2006**, *124*, 241104.
- (7) Taylor, G. Studies in Electrohydrodynamics. I. The Circulation Produced in a Drop by Electrical Field. *Proc. R. Soc. London, Ser. A* **1966**, *291*, 159–166.
- (8) Lucassen-Reynders, E. H.; Lucassen, J. In *Interfacial Rheology*; Miller, R., Liggieri, L., Eds.; CRC Press, 2009; pp 39–72.
- (9) Loglio, G.; Pandolfini, P.; Miller, R.; Makievski, A.; Ravera, F.; Liggieri, L. In *Novel Methods to Study Interfacial Layers*; Möbius, D., Miller, R., Eds.; Studies in Interface Science; Elsevier, 2001; Vol. 11; pp 439–483.
- (10) Miller, R.; Aksenenko, E. V.; Fainerman, V. B. Dynamic interfacial tension of surfactant solutions. *Advances in Colloid and Interface Science* **2017**, *247*, 115–129.

- (11) Mhatre, S.; Simon, S.; Sjöblom, J. Methodology to calculate interfacial tension under electric field using pendent drop profile analysis. *Proc. R. Soc. London, Ser. A* **2019**, *475*, 20180852.
- (12) Mhatre, S.; Simon, S.; Sjöblom, J. Experimental Evidence of Enhanced Adsorption Dynamics at Liquid–Liquid Interfaces under an Electric Field. *Anal. Chem.* **2020**, *92*, 12860–12870.
- (13) Mhatre, S.; Vivacqua, V.; Ghadiri, M.; Abdullah, A.; Al-Marri, M.; Hassanpour, A.; Hewakandamby, B.; Azzopardi, B.; B., K. Electrostatic phase separation: A review. *Chem Eng Res Des* **2015**, *96*, 177–195.
- (14) Sjöblom, J.; Mhatre, S.; Simon, S.; Skartlien, R.; Sørland, G. Emulsions in external electric fields. *Advances in Colloid and Interface Science* **2021**, *294*, 102455.
- (15) Mhatre, S.; Thaokar, R. Pin-Plate Electrode System for Emulsification of a Higher Conductivity Leaky Dielectric Liquid into a Low Conductivity Medium. *Ind Eng Chem Res* **2014**, *53*, 13488–13496.
- (16) Busolo, M.; Castro, S.; Lagaron, J.; Krokida, M. K. In *Thermal and Nonthermal Encapsulation Methods*; Krokida, M. K., Ed.; CRC Press: Boca Raton, FL, 2017; p 22.
- (17) Ruwoldt, J.; Subramanian, S.; Simon, S.; Oschmann, H.; Sjöblom, J. Asphaltene fractionation based on adsorption onto calcium carbonate: Part 3. Effect of asphaltenes on wax crystallization. *Colloids Surf., A* **2018**, *554*, 129 – 141.
- (18) Kilpatrick, P. K.; Spiecker, P. M. In *Asphaltene Emulsions.*; Sjö, Ed.
- (19) Mhatre, S.; Simon, S.; Sjöblom, J. Shape evolution of a water drop in asphaltene solution under weak DC electric fields. *Chem. Eng. Res. Des.* **2019**, *141*, 540–549.
- (20) Yang, J.; Yu, K.; Tsuji, T.; Jha, R.; Zuo, Y. Y. Determining the surface dilational

- rheology of surfactant and protein films with a droplet waveform generator. *Journal of Colloid and Interface Science* **2019**, *537*, 547–553.
- (21) Fainerman, V.; Makievski, A.; Miller, R. The analysis of dynamic surface tension of sodium alkyl sulphate solutions, based on asymptotic equations of adsorption kinetic theory. *Colloids Surf., A* **1994**, *87*, 61 – 75.
- (22) Eastoe, J.; Dalton, J. S. Dynamic surface tension and adsorption mechanisms of surfactants at the air–water interface. *Adv. Colloid Interface Sci.* **2000**, *85*, 103 – 144.
- (23) Torza, S.; Cox, R. G.; Mason, S. G. Electrohydrodynamic deformation and burst of liquid drops. *Phil. Trans. R. Soc. Lond.A* **1971**, *269*, 295–319.
- (24) Ha, J.-W.; Yang, S.-M. Deformation and breakup of Newtonian and non-Newtonian conducting drops in an electric field. *Journal of Fluid Mechanics* **2000**, *405*, 131–156.
- (25) Freer, E. M.; Radke, C. J. Relaxation of asphaltenes at the toluene/water interface: Diffusion exchange and surface rearrangement. *J. Adhesion* **2004**, *80*, 481–496.
- (26) Lucassen-Reynders, E. H.; Cagna, A.; Lucassen, J. Gibbs elasticity, surface dilational modulus and diffusional relaxation in nonionic surfactant monolayers. *Colloids and Surfaces A: Physicochemical and Engineering Aspects* **2001**, *186*, 63–72.
- (27) Chesters, A. The modelling of coalescence processes in fluid-liquid dispersions : a review of current understanding. *Chem Eng Res Des* **1991**, *69*, 259–270.
- (28) Mhatre, S.; Deshmukh, S.; Thaokar, R. T. Electrocoalescence of a drop pair. *Phys. Fluids* **2015**, *27*, 092106.

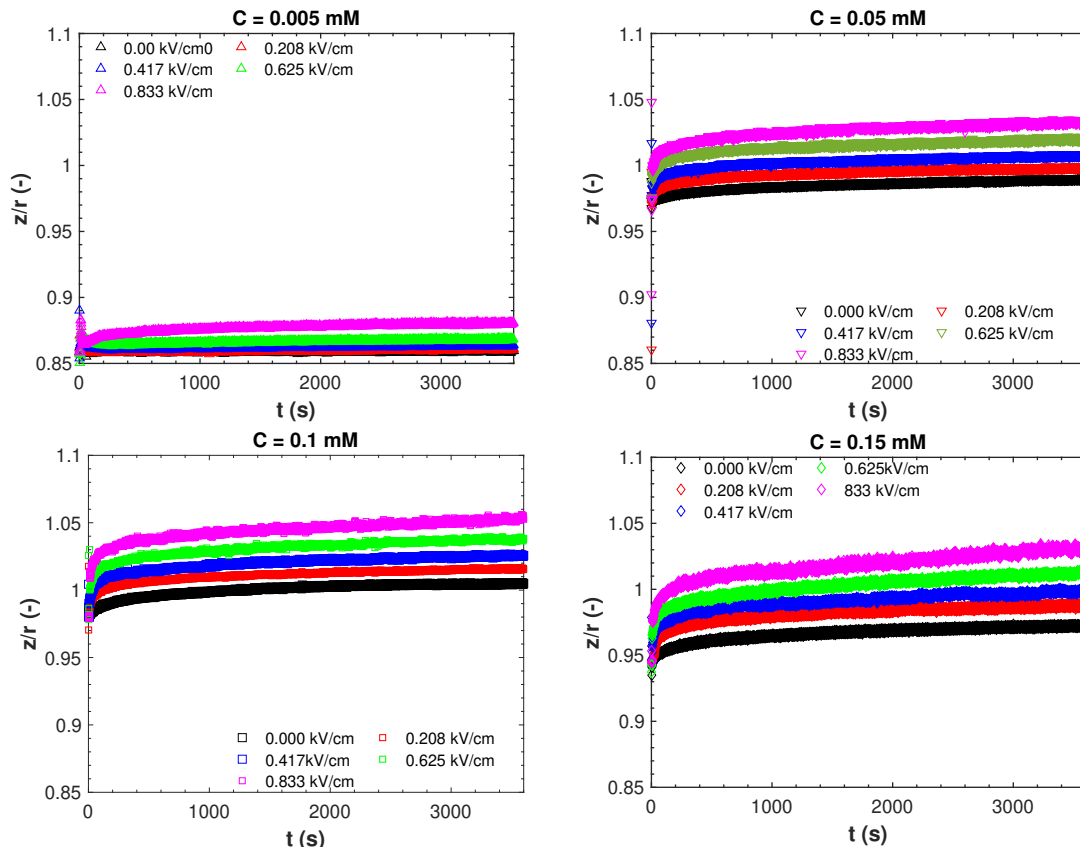


Figure .1: Stretching of a steady pendent water drop in asphaltene-rich organic phase under dc electric fields. z and r are vertical and horizontal axes lengths of the drop respectively.

Drop deformation

Theoretical and experimental $|E|$

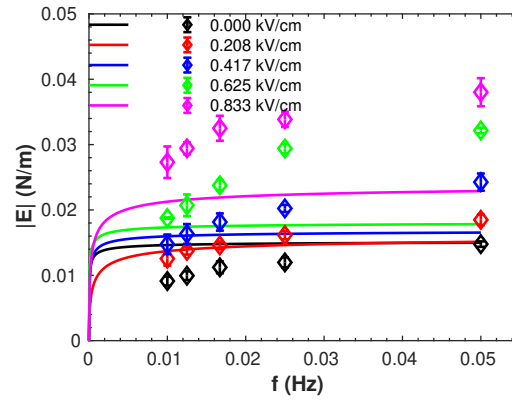


Figure .1: Comparison between experimental(symbols) and theoretical (solid curves) total interfacial moduli ($|E|$) in 0.15 mM solution under electric fields.

Theoretical E' and E'' moduli

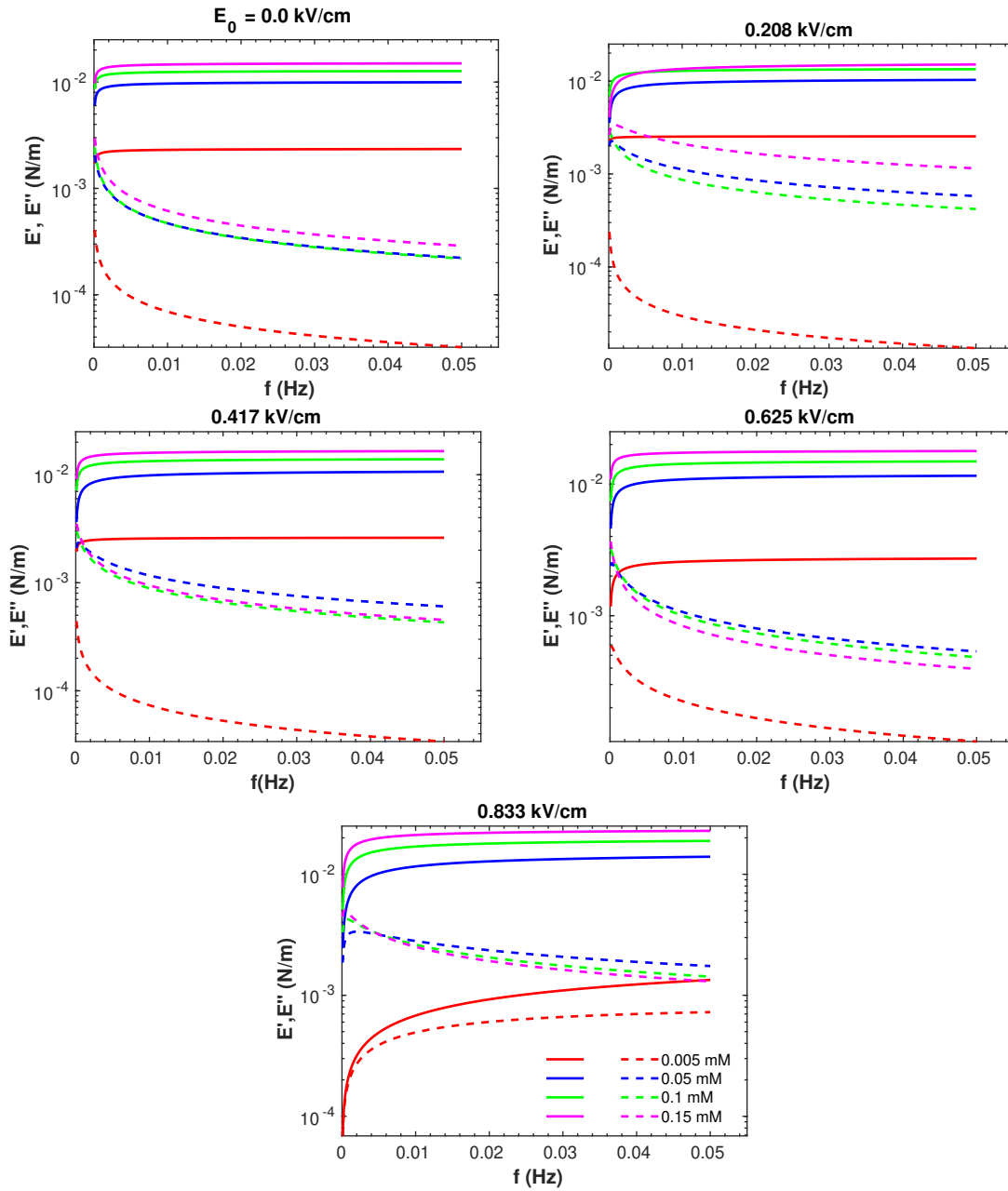
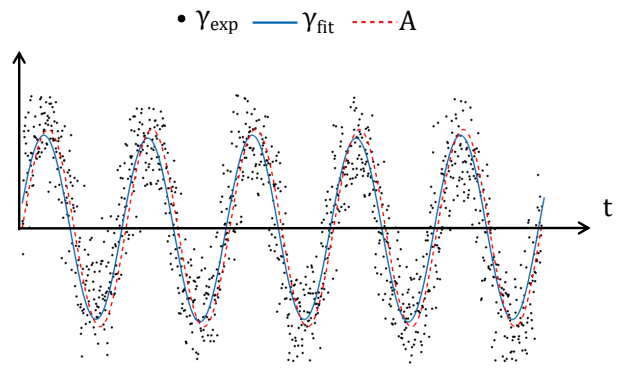
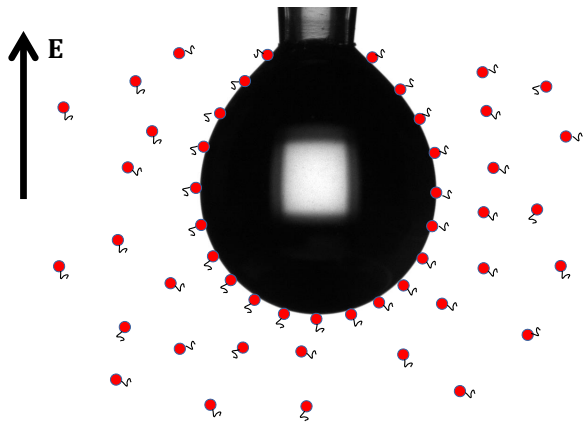


Figure .1: LVDT model estimates for dilational elastic (E') and viscous (E'') moduli of asphaltene films in different concentration bulk phases under external dc electric fields.



For Table of Contents Use Only